# Distinguishing ice β-XV from deep glassy ice VI: Raman spectroscopy

Alexander V. Thoeny, [ID] Tobias M. Gasser [ID] and Thomas Loerting [ID] *

The nature of the hydrogen sublattice of an HCl-doped ice VI sample after cooling at 1.8 GPa has been a topic of recent interest. The samples are interpreted either as the new H-ordered ice phase ice β-XV with a thermodynamic stability region in the phase diagram [T. M. Gasser *et al.*, *Chem. Sci.*, 2018, **9**, 4224], or alternatively as H-disordered, deep glassy ice VI [A. Rosu-Finsen and C. G. Salzmann, *Chem. Sci.*, 2019, **10**, 515]. Here we provide a comprehensive Raman spectroscopic study on ice β-XV, ice XV and ice VI, with the following key findings: (i) the Raman spectra of ice β-XV differ fundamentally from those of ice VI and ice XV, where the degree of H-order is even higher than in ice XV. (ii) Upon cooling ice VI there is competition between formation of ice XV and ice β-XV domains, where ice XV forms at 0.0 GPa, but ice β-XV at 1.8 GPa. Domains of ice β-XV are present in literature "ice XV" at 1.0 GPa. This result clarifies the puzzling earlier observation that the degree of H-order in ice XV apparently improves upon heating and recooling at ambient pressure. In reality, this procedure leaves the H-order in ice XV unaffected, but removes ice β-XV domains by transforming them to ice XV. (iii) Upon heating, the samples experience the transition sequence ice β-XV → ice XV → ice VI, *i.e.*, an order–order transition at 103 K followed by an order–disorder transition at 129 K. The former progresses *via* a disordered transient state. (iv) D$_2$O ice β-XV forms upon cooling DCl-doped D$_2$O-ice VI, albeit at a much lower pace than in the hydrogenated case so that untransformed D$_2$O ice VI domains are present even after slow cooling. The librational band at 380 cm$^{-1}$ is identified to be the characteristic spectroscopic feature of deuterated ice β-XV. Taken together these findings clarify open questions in previous work on H-ordering in the ice VI lattice, rule out a glassy nature of ice β-XV and pave the way for a future neutron diffraction study to refine the crystal structure of D$_2$O ice β-XV.

## Introduction

Polymorphism in H$_2$O-ices is intimately linked with hydrogen and oxygen atom order.[1–7] An ice polymorph may transform from an H-disordered high-temperature variant to its H-ordered low-temperature proxy, while the network of O-atoms is barely affected.[8] Ice VI is one of the high-pressure, H-disordered polymorphs, which is stable at 0.6–2.2 GPa.[9] Ice VI may transform to its H-ordered pendant ice XV, *e.g.*, upon cooling at 1.0 GPa below 129 K.[10] In pure water samples this transformation is so slow that it usually does not occur due to lack of time.[5,11] Under such conditions ice VI is kinetically stable and would transform to ice XV over an infinite period of time. This state of ice VI is then called a "glassy state". This term is misleading, though. The O-atoms are in their crystal lattice positions, so that ice VI is in fact not a glass, but a crystal. This crystal is frustrated in terms of the orientations of the water dipoles. That is, only the H-atoms fulfil the criteria for a glass: they are kinetically arrested in a

disordered arrangement. This frustrated crystal can be avoided by introducing minute amounts of HCl substitutionally into the ice lattice. HCl as a dopant accelerates the reorientation of the dipoles by up to 5 orders of magnitude,[12] thereby allowing the water dipoles to align upon cooling. Other dopants turned out to be less efficient.[13] In the case of ice VI use of HCl as a dopant and cooling experiments on the time scale of minutes have allowed the frustration to be released and ice XV to be produced, which is ordered both in terms of the H- and O-atom positions.[4] Below 129 K ice XV can be kept either as a stable phase at high-pressure conditions (see the phase diagram in Fig. 1) or as a metastable phase also outside its stability domain. Most notably, it can be recovered to 1 bar and stored in liquid nitrogen. Above 129 K the H-atoms in ice XV disorder again, converting it back to ice VI. In other words, the order–disorder transition temperature $T_{o–d}$ of ice XV is 129 K, both at 1.0 GPa and at ambient pressure.[5,14]

An interesting phenomenon was observed by heating ice XV at (sub)ambient pressure from 77 K to $T < T_{o–d}$, followed by recooling to liquid nitrogen temperature.[1,5,14,15] While for all other H-ordered ices the degree of order is not affected upon

*Institute of Physical Chemistry, University of Innsbruck, Innrain 52c,*
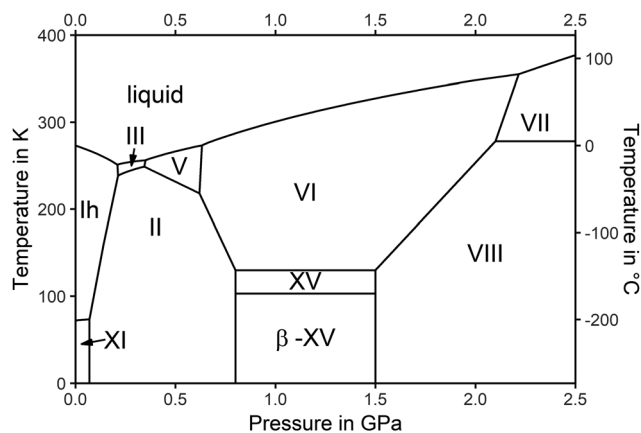*A-6020 Innsbruck, Austria. E-mail: thomas.loerting@uibk.ac.at*

**Fig. 1** Phase diagram, including the stability range of ice β-XV.

heating to $T < T_{o–d}$, the degree of order is enhanced in the case of ice XV.[1,5,11,14,16] Also, the calorimetry signature of ice XV upon heating is different from all other H-ordered ices. The latter show merely a single endothermic event upon heating, which is associated with the disordering at $T_{o–d}$.[5] Ice XV, however, displays a sequence of two endothermic events separated by an exothermic event, indicating that a sequence of H-disordering and ordering processes takes place. This complex thermal behaviour may be caused by the structure of ice VI consisting of two interpenetrating oxygen networks.[17,18] In ref. 5, this behaviour is rationalized as follows: "Migrating point defects, which are thought to be responsible for the hydrogen ordering, are very unlikely to 'jump' from one network to the other. The two networks should therefore have some freedom, at least during the early stages of the phase transition, to hydrogen order independently. Consistent with this scenario, dielectric measurements by Johari et al. on pure ice VI suggested that the onset of hydrogen ordering is ferroelectric". In other words, there is an interplay between two networks, which may order in different ways. Thereby, one has to keep in mind that such a ferroelectric hydrogen ordering would oppose the antiferroelectric hydrogen ordering of ice XV.[10,14] Indeed, calculations reveal that there is close competition between the structure with the strongest local hydrogen bonding (ferroelectric $Cc$ structure)[19] and the one with the most favorable "delocalized" hydrogen bond cooperativity effects (antiferroelectric $P\bar{1}$ structure).[20,21] Raman spectra calculated for the antiferroelectric structure by DFT[14] are "in essential agreement with experimental spectra of ice XV", and so are the calculated structures for this structure by MB-MD.[22]

This explanation leaves some room for speculation, which prompted Gasser et al. to investigate the influence of pressure and cooling rate on H-ordering quantitatively and systematically.[1] By combining X-ray, differential scanning calorimetry (DSC), Raman- and dielectric relaxation spectroscopy experiments they identified a different cause for the complex behaviour that was not observed for any other ice polymorph before. They made the case for another H-ordered variant in the O-lattice of ice VI.[1] Also in this new form of ice the water dipoles are aligned – however, the alignment follows a different pattern than the one known in ice XV. Gasser et al. called this previously unknown polymorph ice β-XV, and it might represent the ferroelectric form identified by Johari and Whalley[11] at the onset of the ordering process. The key observations to make this case are the first endotherm in calorimetry traces, a shift of the (102) Bragg peak in ice VI to higher $d$-spacings for ice XV, but to lower $d$-spacings for the new polymorph, and an activation energy for dielectric relaxation of $\approx 45$ kJ mol$^{-1}$ for ice β-XV, roughly double the one of ice XV.[1] The complex thermal behaviour upon heating is explained on the basis of the transition sequence ice β-XV → ice XV → ice VI by Gasser et al.[1] The two endotherms in the calorimetry trace can then be interpreted to represent, first, the order–order transition ice β-XV → ice XV at $T_{o–o} \approx 103$ K and, second, the previously known order–disorder transition ice XV → ice VI at $T_{o–d} \approx 129$ K. The previously unnoticed existence of the transition at 103 K is the reason why the degree of order in ice XV is affected upon heating to temperatures $T_{o–o} < T < T_{o–d}$ and recooling to $T < T_{o–o}$.

Based on this transition sequence and the change of the configurational entropy as quantified from the size of the endotherms a higher degree of H-order is inferred for ice β-XV than for ice XV.[1] In agreement with this the Raman spectra of ice β-XV show more substructure than the ones of ice XV.[1] Consequently, Gasser et al. claim ice β-XV to be the thermodynamically stable phase in the phase diagram below 103 K in the pressure range 0.8–1.5 GPa as indicated in Fig. 1. For kinetic reasons, however, ice β-XV has to be synthesized by cooling ice VI in the stability range of ice VIII, at 1.8 GPa.[1] Gasser et al. have conjectured that the type of alignment of water dipoles might be ferroelectric, contrary to the antiferroelectric[10] nature of ice XV, without definite proof for this statement. Kuo and Kuhs[23] and Komatsu et al.[24] have listed a total of 45 types of alignment obeying the Bernal–Fowler rules, many of them energetically very close to each other.[18,19,23,24] Ice β-XV is thus the first experimental realization of a second type of water dipole alignment in a given O-lattice, and the first example of an order–order transition in the H-subnetwork in the history of ice research.

Recently, however, Rosu-Finsen and Salzmann reinterpreted ice β-XV to be a "deep glassy state of ice VI", i.e., H-disordered rather than ordered.[16,25] Moreover, they state that high pressures would hamper H-ordering in ice VI such that it is possible to prepare ice XV at 1.0 GPa, but not at 1.8 GPa – which is the pressure used to prepare ice β-XV. They reinterpreted the first endotherm observed by Gasser et al. to mark an orientational glass transition in "glassy" ice VI rather than the order–order transition. They argue that the influence of pressure, heating rate and annealing on the transition is consistent with the expectations for a glassy sample. Thereby, less H-order is gained upon cooling ice VI at higher pressures – which is the exact opposite of the claim by Gasser et al. Furthermore, Rosu-Finsen and Salzmann provide neutron diffraction patterns of deuterated samples that do not show any difference to ice VI. They use this observation to confirm the deep glassy state nature.[16] In their terminology the transition sequence upon heating involves a glass transition from deep glassy ice VI to ice VI at 103 K and the ice XV → ice VI transition at 129 K. The different viewpoints were recently highlighted in an article,[26] in

This journal is © the Owner Societies 2019

*Phys. Chem. Chem. Phys.*, 2019, **21**, 15452–15462 | **15453**

which Dennis D. Klug states in conclusion that "in understanding the properties of water and water ice structures" both groups have "made a significant contribution to the field", where "the search for new ice structures will definitely continue".

All of the arguments presented in favour of deep glassy ice VI are based on DSC measurements. Gasser's results from X-ray diffraction and Raman spectroscopy are, however, barely addressed by Rosu-Finsen and Salzmann and the results from dielectric relaxation spectroscopy are completely left out.[1,16] Neither the different activation energies of ice VI compared to ice β-XV nor the differences between ice VI and β-XV in Raman spectra and X-ray patterns are explained by Rosu-Finsen and Salzmann. The main target of the present work is to provide an interpretation that explains all observations. The key to distinguish between the two different interpretations is the transformation of the "new phase" to ice XV at 103 K. It can be used as a starting point in that process as a glassy state of ice VI is supposed to transform in a different way than ice β-XV. While H-ordered ice β-XV would H-disorder,[1] a deep glassy state of ice VI would either H-order above 103 K or just remain disordered.[16] The H-ordering process of the glassy state is analogous to cold-crystallization of a glass upon heating.

We here look at that issue from a Raman spectroscopic point of view. Raman spectroscopy is especially suitable for identifying a deep glassy or crystalline phase as spectra of H-ordered/H-disordered phases are clearly distinguishable. Over the last 30 years, spectra of the disorder–order pairs ice I/XI,[27,28] V/XIII,[29] VI/XV[14] and XII/XIV[30] have been published. In all these studies, the spectra of the H-ordered phases show more sub-structure and narrower bands. In ice XI, *e.g.*, a sharp one appears at 630 cm$^{-1}$ that does not have an equivalent in its H-disordered proxy ice I.[27] In ice XIII, six narrow OD-stretching bands appear but only a single broad one with two shoulders in H-disordered ice V.[29] The librational band of ice XIV consists of four narrow bands, but that of H-disordered ice XII of a single one with a very broad shoulder.[30] The development of band substructure upon heating is for this reason a key feature allowing one to distinguish the two interpretations. Furthermore, it is the goal to explain why ice XV behaves so differently from all other H-ordered ices upon heating.

# Experimental section

### Sample preparation

Ice β-XV samples are prepared exactly as outlined in Gasser *et al.*[1] In short, HCl-doped ice VI is cooled at 1.8 GPa at 3 K min$^{-1}$ to 80 K. Ice XV samples are prepared as outlined by Shephard and Salzmann.[5] That means HCl-doped ice VI is quenched at 1.0 GPa at ≈40 K min$^{-1}$ to 80 K. Both for ice XV and ice β-XV the hydrogen ordering process takes place at high-pressure conditions. The samples are then recovered to ambient pressure and stored in liquid nitrogen.

The hydrogen-order in these samples is affected by heating and recooling at (sub)ambient pressure. Such samples are referred to as "recooled". Recooled samples are prepared in

this work by heating and subsequently cooling recovered samples at $1.0 \times 10^{-6}$ GPa (10 mbar, 7.6 Torr) inside the Raman cryostat. Obviously, the temperature to which "recooled samples" were heated and at what rate the recooling was done are of key importance. To clearly specify what was done we use the nomenclature "ice XV$_{rec(135K,\ 20K\,min^{-1})}$" here. This describes an ice XV sample that was heated at $1.0 \times 10^{-6}$ GPa to 135 K and then recooled with a cooling rate of 20 K min$^{-1}$. In cases where the cooling rate is not mentioned it is our standard cooling rate of 2 K min$^{-1}$.

In addition, we also use a nomenclature that specifies the pressure (in GPa) at which the samples were cooled. Samples recooled at $1.0 \times 10^{-6}$ GPa are called "ice XV$_{0.0GPa}$" in this terminology, whereas samples cooled at 1.0 GPa are called "ice XV$_{1.0GPa}$". This nomenclature is useful to clarify the impact of pressure on the sample nature.

### Raman experiments

Raman spectra were taken using a WITec WMT50 Raman microscope including a laser of a wavelength of 532 nm and a maximal power output of 20 mW with a ZEISS LD Plan-NEOFLUAR/40×-objective. The quench-recovered samples were powdered under liquid nitrogen and then transferred into an Oxford N Microstat, which was precooled to 84 K and coupled to the microscope. During the measurement it was evacuated to $1.0 \times 10^{-6}$ GPa. The temperature was controlled by a Lakeshore 331S temperature controller. For each spectrum, the integration time was set to 28 min. The spectra were collected using an 1800 g mm$^{-1}$ grating and a CCD-camera.

Analogously to previous Raman-studies,[14,29,30] deionized H$_2$O mixed with 5 wt% D$_2$O was used to prepare the samples. That provides the possibility to measure decoupled OD-stretching bands in addition to coupled OH-stretching bands. They are more convenient to describe H-bonding than coupled OH-bonds and can, therefore, better be distinguished by substructure.[30]

# Results

### Section 1: comparison of the Raman spectra of ice β-XV with ice XV$_{rec(120K)}$ and ice VI at 84 K

The first task is to identify the spectroscopic features distinguishing ice β-XV, ice XV and ice VI, *i.e.*, to demonstrate the spectroscopic features distinguishing the three types of H-(dis)order in the O-lattice of ice VI. Since recooled ice XV was shown to be more ordered than ice XV$_{1.0GPa}$[14] we here use ice XV$_{rec(120K)}$ to represent ice XV. Thus, in Fig. 2, ice β-XV is compared with ice VI and ice XV$_{rec(120K)}$. Fig. 2 here is similar to Fig. 8 in Gasser *et al.*[1] The only difference between these two figures is that we here show spectra for an ice XV$_{rec(120K)}$ sample instead of the ice XV$_{rec(130K)}$[1] sample used in our earlier work. Ice XV is claimed to be of the highest H-order when prepared as ice XV$_{rec(120K)}$.[31]

Within all spectral ranges ice β-XV shows more substructure and narrower bands than ice VI. Especially the substructure of the OD- and translational bands is more pronounced in β-XV than that in ice VI. A relatively well resolved band of medium
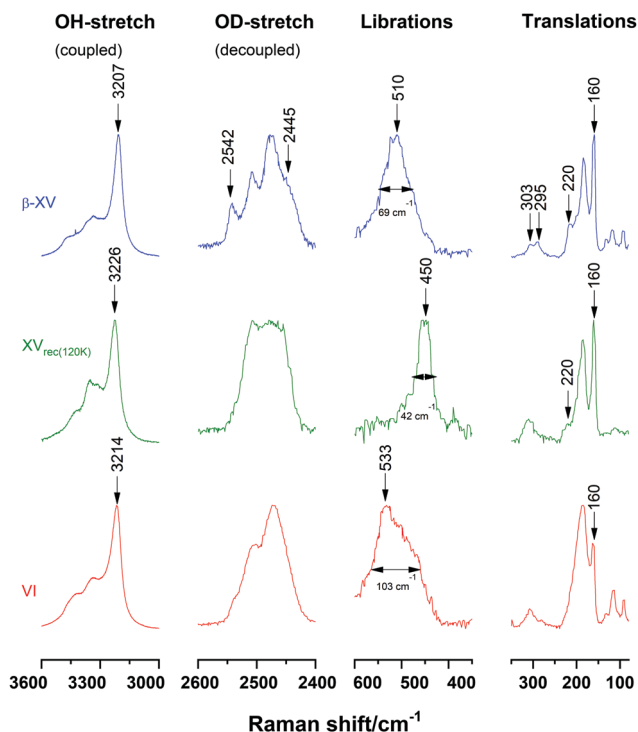
15454 | *Phys. Chem. Chem. Phys.*, 2019, **21**, 15452–15462

This journal is © the Owner Societies 2019

**Fig. 2** Comparison of Raman spectra of ice β-XV (blue), ice XV$_{rec(120K)}$ (green) and ice VI (red). Spectra were normalized for matching intensities of the most intense band in each range.

intensity occurs at 2542 cm$^{-1}$ in the spectra of ice β-XV whereas for ice XV or VI at most a slight shoulder appears at that position (marked by an arrow in Fig. 2). Moreover, the shoulder at 2445 cm$^{-1}$ appears in ice β-XV, but not in ice VI or XV$_{rec(120K)}$. In the translational range, the band at 220 cm$^{-1}$ appears in both ice XV$_{rec(120K)}$ and ice β-XV, but not in ice VI (marked by an arrow). This translational band is especially interesting, as it has been used as an indication of H-ordering by Whale et al.[14] The intensity of this band increases from ice VI to ice XV and ice β-XV. This immediately suggests a higher degree of H-order in ice β-XV than in ice XV. If ice β-XV was a deep glassy ice VI phase as suggested by Rosu-Finsen and Salzmann, the band at 220 cm$^{-1}$ would need to be absent, just like in the ice VI reference (marked by an arrow in Fig. 2). Furthermore, band splitting at 303 cm$^{-1}$ and 295 cm$^{-1}$ appears exclusively in ice β-XV (marked by two arrows).

Ice β-XV can also be distinguished from ice VI by features of the librational spectra. The librational band of ice XV$_{rec(120K)}$ centred at 450 cm$^{-1}$ differs a lot from both ice β-XV and ice VI: it is redshifted by 83 cm$^{-1}$ and 60 cm$^{-1}$, respectively. Comparing the librational band for ice VI and ice β-XV, its FWHM decreases from 103 cm$^{-1}$ to 69 cm$^{-1}$ and its position shifts from 533 cm$^{-1}$ to 510 cm$^{-1}$. That is, the position and the FWHM of the librational band are well suited to distinguish different types of H-order and H-disorder. Additional distinctive features are found in other spectral ranges: the bands of ice β-XV are narrower in the OH-stretching, OD-stretching and translational spectral range compared to ice VI. Moreover, the OH-stretch band at 3207 cm$^{-1}$ in ice β-XV is shifted both

against ice XV and ice VI. All these observations are evidence for a large degree of H-order in ice β-XV and evidence against ice β-XV being an H-disordered, glassy state very similar to ice VI. These differences set ice β-XV apart from both ice XV and ice VI. The appearance of additional bands in the OD-stretching region implies that the unit cell of ice β-XV contains crystallographically distinct water molecules that are not present in ice VI or XV.

That is, the spectra depicted in Fig. 2 make a strong case for three distinct phases in the O-network of ice VI. If ice β-XV was instead deep glassy ice VI then only two distinct sets of spectra would be observed. One could argue that Fig. 2 shows two distinct sets of spectra, and the ice β-XV spectrum represents a superposition of the other two. This possibility can be clearly ruled out. There is no way that the OH-stretching band at 3207 cm$^{-1}$ in ice β-XV can be expressed as a linear combination of the two OH-stretching bands at 3214 and 3226 cm$^{-1}$ in ice VI and ice XV, respectively. Also, the additional bands in the OD-stretching region cannot be explained based on a superposition. The spectra of ice β-XV cannot be expressed as a superposition of ice XV$_{rec(120K)}$ and ice VI. That contradicts ice β-XV being a mixture of ice VI and XV$_{rec(120K)}$ as it would be assumed for a mixture of deep glassy ice VI and ice XV.

**Section 2: the influence of pressure**

Gasser et al. showed in DSC experiments that the latent heat associated with the transition at 103 K increases with pressure.[1] This transition is assigned as the ice β-XV → ice XV transition by Gasser et al., but as the glass transition of a deep glassy state of ice VI by Rosu-Finsen and Salzmann. According to Rosu-Finsen and Salzmann, pressure hinders the H-ordering process. Thereby, endothermic overshoots that are not related to latent heat grow with increasing pressure.[16] By contrast, Gasser et al. claim that an increase in pressure promotes H-ordering.[1]

Fig. 3a compares an ice XV sample cooled to $T < 103$ K at 1.0 GPa with ice XV recooled at $1.0 \times 10^{-6}$ GPa as well as with ice β-XV cooled at 1.8 GPa. Using now the pressure of synthesis in units GPa as a label, at which the cooling to $T < 103$ K took place, these samples are then called ice XV$_{1.0GPa}$, ice XV$_{0.0GPa}$ and ice β-XV$_{1.8GPa}$, respectively. Obviously, ice XV$_{1.0GPa}$ features broader librational bands than both ice XV$_{0.0GPa}$ and ice β-XV$_{1.8GPa}$. That is in line with Whale et al.'s observation of ice XV$_{0.9GPa}$ having broader bands than ice XV$_{0.0GPa}$ samples recooled at $1.0 \times 10^{-6}$ GPa.[12] Specifically, the half-widths at half maximum are $37 \pm 12$ cm$^{-1}$ and $66 \pm 12$ cm$^{-1}$ for the recooled 0.0 GPa and 1.8 GPa samples, but $107 \pm 25$ cm$^{-1}$ for the 1.0 GPa samples. The half-width for ice XV$_{1.0GPa}$ is larger especially because there is a broad shoulder centred at 510 cm$^{-1}$. This band position exactly matches the one characteristic of ice β-XV (cf. Fig. 2). This shoulder and the much broader librational bands for ice XV$_{1.0GPa}$ than for ice XV$_{0.0GPa}$ and ice β-XV$_{1.8GPa}$ thus suggest the following: at 0.0 GPa antiferroelectric order in ice XV is found upon cooling ice VI. At 1.8 GPa the (ferroelectric?) H-order in ice β-XV is found upon cooling ice VI. At intermediate pressure, e.g., 1.0 GPa, there is competition between the two types of order. One could imagine that domains of both ice XV
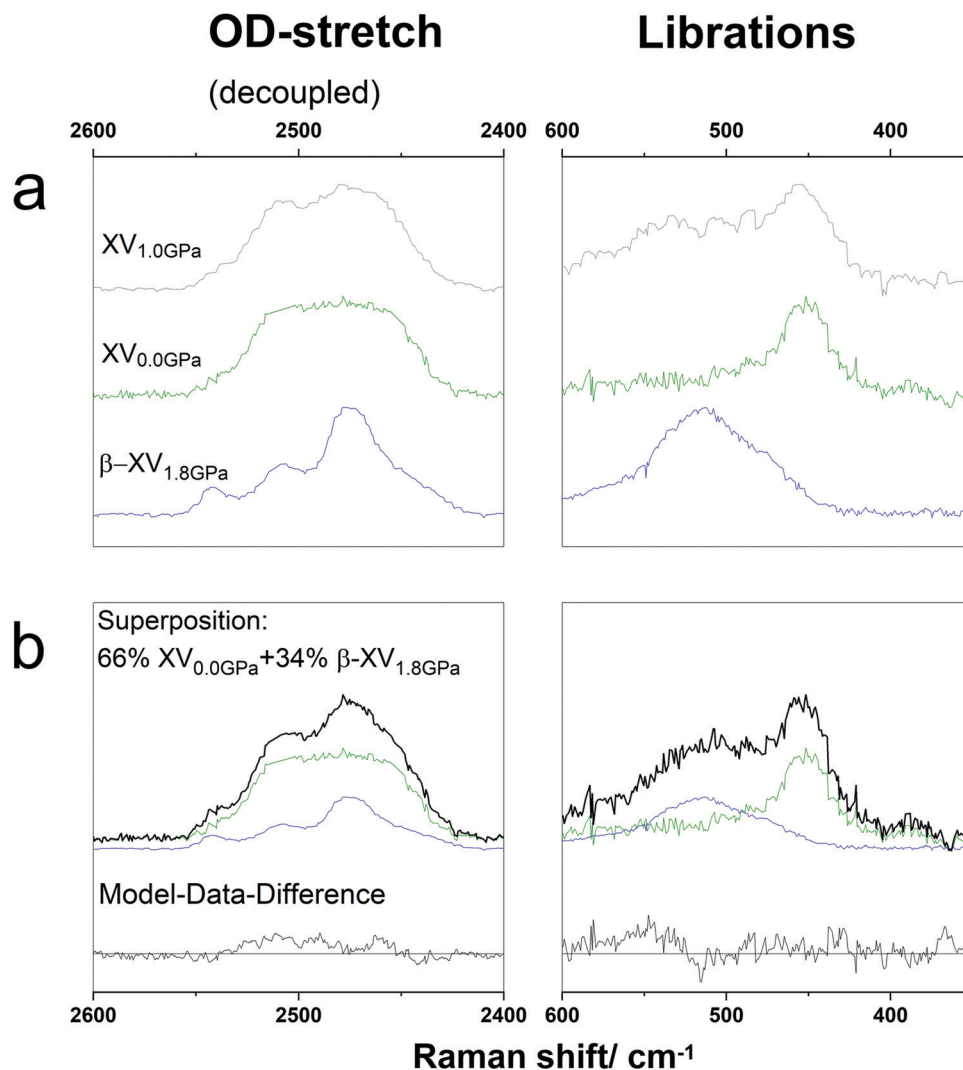
This journal is © the Owner Societies 2019

*Phys. Chem. Chem. Phys.*, 2019, **21**, 15452–15462 | **15455**

**Fig. 3** (a) Comparison of librational- and OD-stretching-bands of ice "XV"$_{1.0GPa}$ with ice β-XV$_{1.8GPa}$ and ice XV$_{0.0GPa}$ and (b) reconstruction of the ice "XV"$_{1.0GPa}$ spectra as a superposition of ice XV$_{0.0GPa}$ and ice β-XV$_{1.8GPa}$. Spectra were normalized for matching intensities of the most intense band in each range.

and ice β-XV form upon cooling. This would then imply that ice "XV"$_{1.0GPa}$ can be regarded as a mixture of both ice XV and ice β-XV. The size of each domain has to be much smaller than the laser spot used for the Raman experiment, which has a diameter of $\approx 5$ μm.

To test this hypothesis, we have tried reproducing the ice XV$_{1.0GPa}$ spectra as a superposition of ice XV$_{0.0GPa}$ and ice β-XV$_{1.8GPa}$. A superposition of 66% ice XV$_{0.0GPa}$ and 34% ice β-XV is shown in Fig. 3b. The superposition is a good match, even though the residual model-data difference (bottom of Fig. 3b) is not featureless. By comparison with Fig. 2 the difference is identified as a small contamination with ice VI. This analysis suggests that ice XV$_{1.0GPa}$ contains about 1/3 ice β-XV-domains and 2/3 ice XV-domains under the assumption of similar cross-sections for both domains. That also manifests in the decoupled OD-stretching mode. Ice XV$_{1.0GPa}$ shows a shoulder at 2539 cm$^{-1}$ and a weakly resolved band at 2509 cm$^{-1}$. Both these features are seen with a much better resolution in the β-XV$_{1.8GPa}$-spectrum, but not resolved in ice XV$_{0.0GPa}$.

This conclusion of ice "XV"$_{1.0GPa}$ containing about 2/3 ice XV and 1/3 ice β-XV also explains the size of the endotherms in DSC experiments.[1,16] Gasser et al. as well as Rosu-Finsen and Salzmann showed that the size of the first endotherm increases continuously with the synthesis-pressure. The size of the first endotherm was given as 9 J mol$^{-1}$ at 1.0 GPa and 48 J mol$^{-1}$ at 1.8 GPa in Fig. 2 of ref. 1. Attributing the first endotherm to the ice β-XV → ice XV transition and assuming the 1.8 GPa sample to be 100% ice β-XV, the 1.0 GPa sample contains a fraction of 9/48 ($\approx 20$%) ice β-XV. The difference between $\approx 34$% ice β-XV domains in ice XV$_{1.0GPa}$ deduced from Raman and $\approx 20$% deduced from calorimetry is experimental error. Assuming an error bar of $\pm 5$ J mol$^{-1}$ in the latent heat the calorimetry result is $20 \pm 15$%, which is consistent with 1/3 ice β-XV domains contained in ice XV$_{1.0GPa}$. In other words, as the synthesis pressure increases the fraction of ice β-XV domains increases continuously, concomitantly with the increase of the size of the endotherm in Fig. 2 of ref. 1. There is competition between the two types of order, where an increase in pressure

favours ice β-XV. Analogously, a decrease in pressure favours ice XV domains.

These considerations also explain why it was observed previously[14,16] that H-order in ice XV increases after recooling from 120 K at 0.0 GPa. In essence, the domains of ice β-XV occupying 1/3 of the ice "XV"$_{1.0GPa}$ sample are heated beyond their order–order temperature $T_{o–o}$ of 103 K, transforming them to ice XV domains. Upon recooling the pressure is not sufficient to reform ice β-XV, but ice XV is maintained. Also untransformed ice VI domains that might be part of the sample transform to ice XV upon recooling. That is, recooling at ambient pressure from temperatures above $T_{o–o} \approx 103$ K, but below $T_{o–d} \approx 129$ K, removes ice β-XV domains as well as ice VI domains. This explains why recooling from $T < T_{o–d}$ has only an effect on ice XV, but not on any other H-ordered ice phase.

## Section 3: ice β-XV upon heating

As mentioned in the introduction, one possibility to distinguish ice β-XV from a deep glassy state of ice VI is its behaviour upon heating. Gasser *et al.* suggest a transition of ice β-XV into ice XV at 103 K and then to ice VI at 129 K.[1] Rosu-Finsen and Salzmann on the other hand claim that the deep glassy state of ice VI devitrifies and crystallizes above the glass transition temperature near 103 K into the more stable ice XV, which in turn transforms back into ice VI at 129 K.[16] Based on these two differences, a criterion can be defined to distinguish between deep glassy ice VI and ice β-XV. Whereas Rosu-Finsen and Salzmann expect a sequence deep glassy VI $\xrightarrow{103 \text{ K}}$ XV $\xrightarrow{129 \text{ K}}$ VI involving two phases,[16] Gasser *et al.* expect the sequence β-XV $\xrightarrow{103 \text{ K}}$ XV $\xrightarrow{129 \text{ K}}$ VI including three phases.[1]

Fig. 4 shows the development of ice β-XV spectra upon heating. One can clearly distinguish three different spectra representing three different phases occurring during that process. They are shown in blue (ice β-XV), green (ice XV) and red (ice VI). Grey spectra represent mixed phases. For further discussion, closer consideration of single significant features is necessary.

The peak-area-ratio of the band at 220 cm$^{-1}$ compared to that at 160 cm$^{-1}$ has been introduced as an indicator of H-ordering by Whale *et al.*[14] Therefore, both of these bands were fitted as Gaussian-peaks and then integrated. This ratio will be referred to as the "Whale-index". The band at 220 cm$^{-1}$ occurs in ice XV but not in ice VI. Whale *et al.* determined a ratio of 0 for ice VI above 129 K, and 0.18 for ice XV below 129 K.[14] For a deep-glassy state of ice VI as suggested by Rosu-Finsen and Salzmann, one would then expect the Whale-index to be 0 as well. Above 103 K, one would expect it to increase to 0.18 and at 129 K to decrease again to 0. Fig. 5a shows the development of that ratio for ice β-XV upon heating. At low temperatures, the ratio is 0.30–0.35 and, thereby, even higher than the ratio of 0.18 shown by Whale *et al.* for ice XV.[14] Between 101 K and 105 K, the ratio drops to 0.15–0.20 and between 125 K and 135 K to 0, implying the transition sequence β-XV → XV → VI. This indicator clearly speaks against H-disordered, deep glassy ice VI below 103 K, but for a higher degree of order than in ice XV.



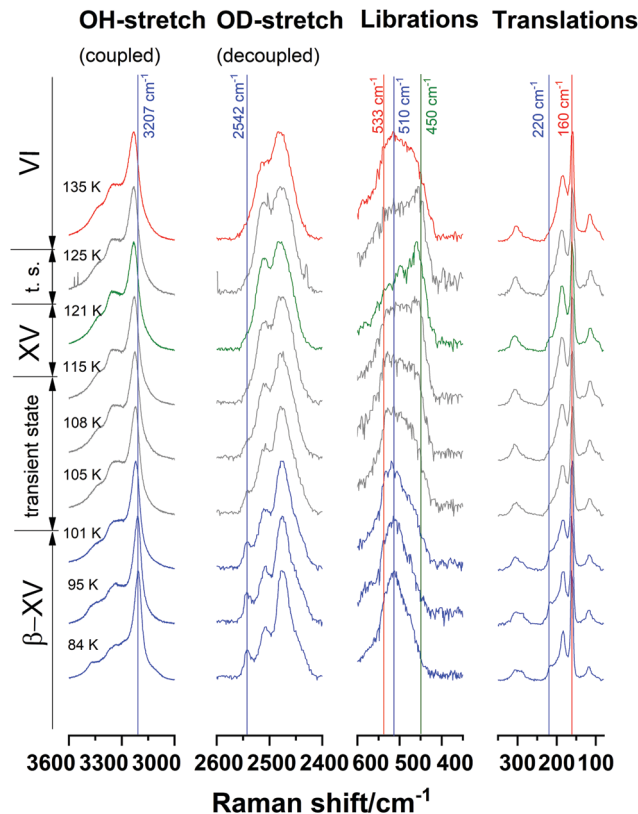**Fig. 4** Raman spectra of ice β-XV upon heating at $1.0 \times 10^{-6}$ GPa. Spectra were normalized for matching intensities of the most intense band in each range. Color code as in Fig. 2, where grey spectra represent transient/mixed states.

As mentioned in Section 1, the band at 2542 cm$^{-1}$ is characteristic of ice β-XV as it neither occurs in ice XV nor in ice VI. This is used here to define another index that we call the "OD-index". Its purpose is to distinguish ice β-XV from ice XV and ice VI. It is not designed to distinguish ice XV and ice VI. More precisely, we define the OD-index as the intensity ratio of the band maximum at 2542 cm$^{-1}$ compared to the minimum at 2530 cm$^{-1}$. Its development upon heating is shown in Fig. 5b. Thereby, blue triangles indicate samples that were originally synthesized as ice β-XV, green circles samples that were synthesized as ice XV$_{rec(120K)}$ and red squares samples that were synthesized as ice VI. At 84 K the OD-index for ice β-XV is in the range of 1.2–1.4 and, thereby, approximately twice the value found for ice VI and thrice the value for ice XV$_{rec(120K)}$. Upon heating ice β-XV the OD-index starts to drop at 100 K and remains distinguishable from the other phases up to 105 K until it converges with them at 108 K. This indicates that ice β-XV progressively transforms between 100 and 108 K, in accordance with the observation of the first endotherm in calorimetry experiments. Ice VI and XV$_{rec(120K)}$, on the other hand, are hardly distinguishable from each other by the OD-index and hardly change during the heating process. In the scenario put forward by Rosu-Finsen and Salzmann, one would expect this ratio to remain constant (either reflecting ice XV or ice VI) in the whole temperature range from 84 K to above 129 K.
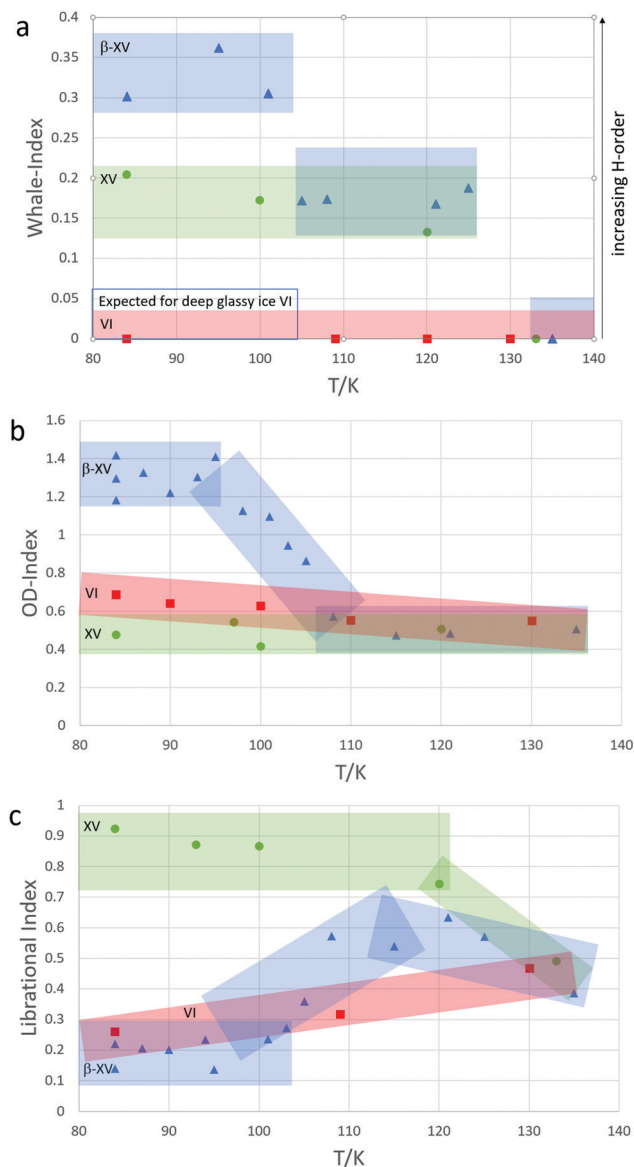
**Fig. 5** Heating process of ice VI, ice XV and ice β-XV. Development of the (a) Whale-index, (b) OD-index and (c) librational index. The coloured symbols represent the nature of the sample at 80 K, namely undoped ice VI-samples (red squares), ice XV$_{rec(120K)}$ (green circles) and ice β-XV (blue triangles).

A third index is required to understand the whole transformation sequence since it is not possible to distinguish between ice XV$_{rec(120K)}$ and ice VI by the OD-index or to distinguish between ice XV$_{rec(120K)}$ and a mixture of ice β-XV and ice VI by the Whale-index. In ref. 1 the "librational index" based on the shape of the librational band has been introduced. The librational band is especially appropriate to distinguish ice XV from both of the other phases as it is redshifted from that of ice β-XV by 60 cm$^{-1}$ and from that of ice VI by 83 cm$^{-1}$. The librational index is defined as the ratio of the intensity at 450 cm$^{-1}$, which is characteristic of ice XV$_{rec(120K)}$, to the integrated intensity at 450 and 510 cm$^{-1}$. Its development is shown in Fig. 5c. The librational index for ice XV$_{rec(120K)}$ at 84 K (green) is approximately

three times higher than the one of ice VI (red) and five times higher than the one of ice β-XV (blue). At higher temperatures, the differences shrink owing to peak broadening. Up to 120 K, however, the values for ice XV remain clearly separated from those for ice VI and ice β-XV. The librational index for ice β-XV increases between 102 and 104 K, which is consistent with ice β-XV transforming at 103 K. At temperatures of 108 K and higher, the librational index of heated ice β-XV lies clearly above that of ice VI, but matches that of ice XV. That implies the occurrence of ice XV in the temperature range of 103 K to 129 K and, therefore, an H-order-to-order transition of ice β-XV to ice XV. Interestingly, the librational index for ice β-XV does not fully rise to the level of ice XV$_{rec(120K)}$ before the onset of the ice XV → ice VI transition. We assume that H-ordered ice β-XV cannot transform directly into H-ordered ice XV but has to pass through an H-disordered transition state instead. In other words, the transition state for the order–order transition has to be disordered. This "transient ice VI" will be addressed in more detail in our future publications.

### Section 4: deuterated ice β-XV: influence of the cooling rate

One of Rosu-Finsen and Salzmann's main arguments in favour of their hypothesis is based on a comparison of DSC measurements and neutron diffraction experiments of a quenched, deuterated DCl-doped 1.8 GPa-sample. As the DSC curves are comparable to those of the hydrogenated samples, they assume a similar nature of the deuterated and hydrogenated sample. The neutron diffraction pattern matches that of ice VI, prompting them to regard the deuterated sample as deep glassy ice VI.[16] As evidenced above in Sections 1–3, the transformation from ice β-XV to ice XV causes the first endotherm in hydrogenated samples rather than the glass transition of deep glassy ice VI followed by crystallization to ice XV. This extrapolation from deuterated to hydrogenated samples needs to be taken with caution, however. In fact, the cooling rate plays a crucial role in this context that has been overlooked.

The importance of the choice of cooling rate is demonstrated in Fig. 6 for hydrogenated ice VI samples cooled at $1.0 \times 10^{-6}$ GPa. Generally, one can expect a lower degree of H-ordering for faster cooling rates. Fig. 6a compares the librational band of samples recooled from 135 K at different rates and one sample recooled from 120 K at 2 K min$^{-1}$. The cooling rates employed differ by a factor of 10, between 2 K min$^{-1}$ and 20 K min$^{-1}$. The librational bands of these samples differ markedly. The relative intensity of the OD-band at 2507 cm$^{-1}$ (not shown in Fig. 6) for ice XV$_{rec(135K, 20 K min^{-1})}$ is smaller than that of ice XV$_{rec(135K, 2 K min^{-1})}$ and the relative intensity at 533 cm$^{-1}$ is remarkably high for ice XV$_{rec(135K, 20K min^{-1})}$. Both of these features suggest a significant fraction of ice VI in ice XV$_{rec(135K, 20K min^{-1})}$. Fig. 6b shows that the ice XV$_{rec(135K, 20K min^{-1})}$ spectrum can be expressed as a superposition of 45% ice XV and 55% ice VI, where the residuals are small, but not featureless. That is, whereas at 2 K min$^{-1}$ ice VI transforms entirely into ice XV, at 20 K min$^{-1}$ roughly half of the ice VI remains untransformed. An analogous behaviour was noted for the ice XIV → XII transformation at (sub)ambient pressure.[30] Exactly this was also observed by Salzmann et al. for the case of the ice V → XIII transformation.[29]

**15458** | *Phys. Chem. Chem. Phys.*, 2019, **21**, 15452–15462
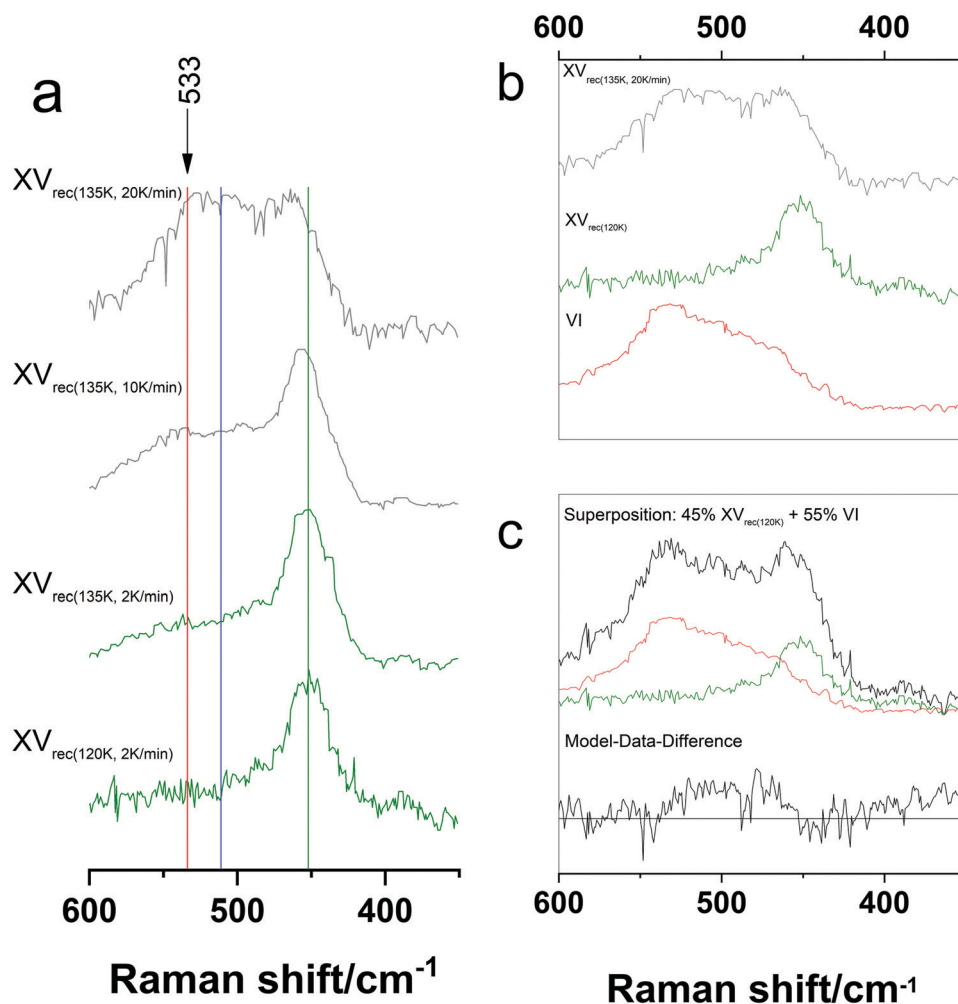
This journal is © the Owner Societies 2019

**Fig. 6** Influence of the cooling rate on the ice VI → XV-transition: (a) librational band, (b) comparison of ice XV$_{rec(135K, 20K min^{-1})}$ with ice VI and ice XV$_{rec(120K)}$ and (c) reconstruction of the ice XV$_{rec(135K, 20K min^{-1})}$ band by a superposition of ice XV$_{rec(120K)}$ and ice VI. Spectra were normalized for matching intensities of the most intense band in each range.

This requirement to provide enough time is of even higher importance for deuterated samples: the process of D-ordering takes place on a different time scale to the process of H-ordering, *i.e.*, several deuterated ices transform more slowly than their hydrogenated counterparts into their respective H-ordered proxies.[32] Consequently, a suitable cooling rate for the formation of deuterated ice β-XV needs to be established.

To this end we compare a DCl-doped deuterated 1.8 GPa-sample that was quenched at a rate of 45 K min$^{-1}$ (D$_2$O-1.8 GPa$_{45 K min^{-1}}$, Fig. 7a, top), mimicking Rosu-Finsen and Salzmann's protocol, with a sample cooled slowly at 1 K min$^{-1}$ under otherwise identical conditions (D$_2$O-1.8 GPa$_{1K min^{-1}}$, Fig. 7c, top). It is immediately evident that the spectra are different. To assess the nature of the D-sublattice we provide reference spectra for deuterated ice VI (Fig. 7a and c, bottom) and XV$_{rec(135K)}$ (Fig. 7a and c, middle). The band position of deuterated ice XV fits the literature value of 338 cm$^{-1}$ exactly. Also, for D$_2$O-ice VI the agreement with an undoped literature sample is good (402 *vs.* 406 cm$^{-1}$).[14]

D$_2$O-1.8 GPa$_{45 K min^{-1}}$ is very similar to the D$_2$O-ice VI reference. In fact, the agreement with the literature D$_2$O-ice VI spectrum is

just as good as with our own reference spectrum. Therefore, it is not surprising that the neutron diffraction pattern published by Rosu-Finsen and Salzmann indicates the sample to be D$_2$O ice VI.[16] This is fully consistent with the experiments presented here.

The situation is different when using a cooling rate of 1 K min$^{-1}$ and thereby providing approximately 50 times more time for the deuterons to order. The librational band of D$_2$O-1.8 GPa$_{1K min^{-1}}$ (Fig. 7c, top) differs from the band of D$_2$O-1.8 GPa$_{45 K min^{-1}}$ and is now located at 380 cm$^{-1}$, between those of D$_2$O-ice XV$_{rec(135K)}$ and D$_2$O-ice VI. Similarly, in hydrogenated samples (see Fig. 2) the librational band of ice β-XV is located between ice XV and ice VI. The occurrence of the band at 380 cm$^{-1}$ might thus be a signature of D$_2$O-ice β-XV. To shed further light on this hypothesis, the librational band positions for the hydrogenated and deuterated samples are compared in Table 1. The isotope effect for librational bands, expressed as ratio of hydrogenated over deuterated band positions, is 1.33. This holds true both for ice VI and ice XV. Similarly, the isotope effect for the librational band of H$_2$O-ice β-XV to that of D$_2$O-1.8 GPa$_{1K min^{-1}}$ is 1.34. This implies that the band at 380 cm$^{-1}$
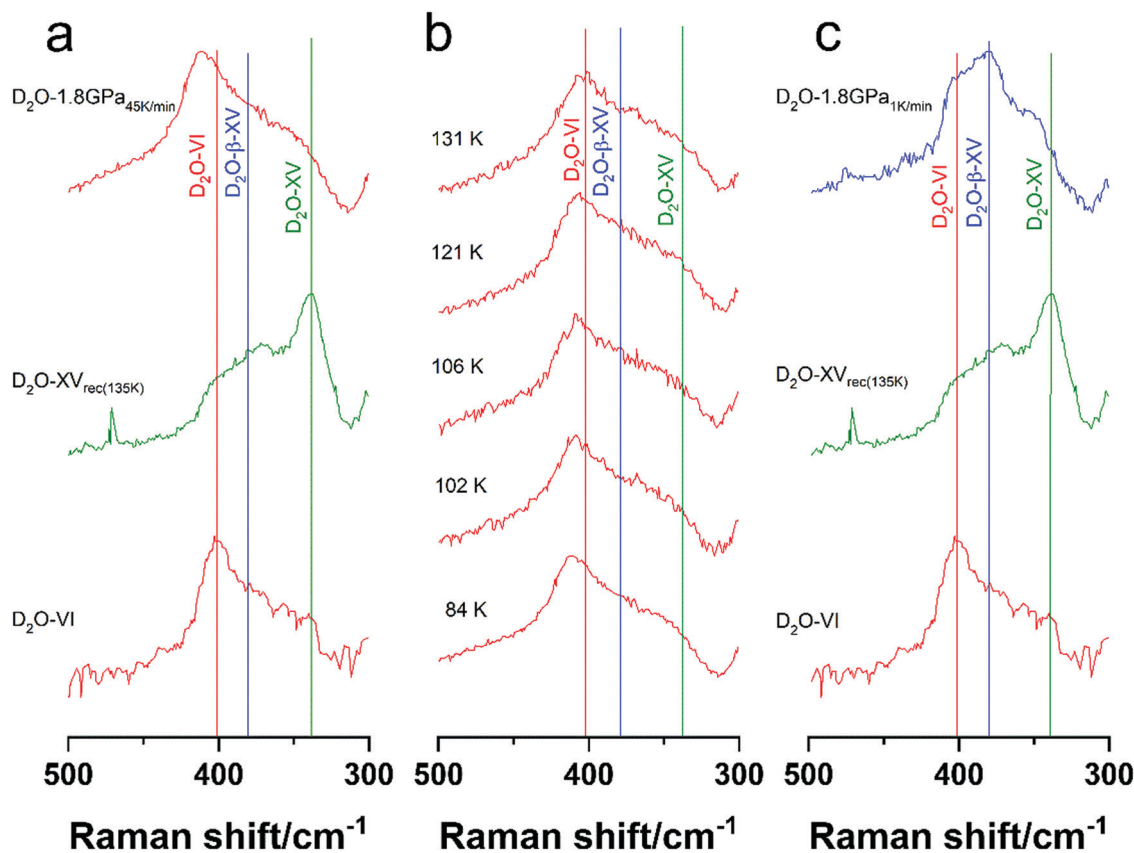
This journal is © the Owner Societies 2019

*Phys. Chem. Chem. Phys.*, 2019, **21**, 15452–15462 | 15459

**Fig. 7** Librational bands of deuterated samples: (a) comparison of $D_2O$-1.8 GPa$_{45\,K\,min^{-1}}$ with $D_2O$-ice VI, and $D_2O$-ice XV$_{rec(135K)}$, (b) $D_2O$-1.8 GPa$_{45\,K\,min^{-1}}$ upon heating and (c) comparison of $D_2O$-1.8 GPa$_{1\,K\,min^{-1}}$ with $D_2O$-ice VI and $D_2O$-ice XV$_{rec(135K)}$. Spectra were normalized for matching intensities of the most intense band in each range.

**Table 1** Position of the librational bands in hydrogenated and deuterated samples

|       | $\nu(H_2O)/cm^{-1}$ | $\nu(D_2O)/cm^{-1}$ | $\nu(H_2O)/\nu(D_2O)$ |
|-------|---------------------|---------------------|------------------------|
| β-XV  | 510                 | 380                 | 1.34                   |
| XV    | 450                 | 338                 | 1.33                   |
| VI    | 533                 | 402                 | 1.33                   |

indicates the presence of $D_2O$-ice β-XV in the $D_2O$-1.8 GPa$_{1K\,min^{-1}}$ sample.

Contrary to hydrogenated ice β-XV-samples, however, $D_2O$-1.8 GPa$_{1K\,min^{-1}}$ shows two shoulders fitting the peak positions of ice XV and ice VI. This indicates that $D_2O$-1.8 GPa$_{1K\,min^{-1}}$ is not composed entirely of deuterated ice β-XV domains, but rather composed of a mixture of $D_2O$-ice β-XV, $D_2O$-ice XV and $D_2O$-ice VI domains. In other words, untransformed ice VI is part of the sample so that cooling rates even lower than 1 K min$^{-1}$ are required to order these domains as well. Therefore, we assume that formation of deuterated ice β-XV, without any by-phase, might require cooling rates clearly slower than 1 K min$^{-1}$ and cooling rates at least 50 times, probably even 500 times, slower than used by Rosu-Finsen and Salzmann. In order to solve the crystal structure for ice β-XV it will be necessary to prepare $D_2O$-ice β-XV as pure as possible, without

contamination of ice XV and ice VI. The Raman data in Fig. 7 show how to achieve this goal. Very slow cooling of DCl-doped $D_2O$ ice VI, possibly over many days, at high-pressure will be required.

As a final point, we look into the development of the $D_2O$-1.8 GPa$_{45\,K\,min^{-1}}$ sample upon heating in Fig. 7b. According to Rosu-Finsen and Salzmann's interpretation of DSC curves, that sample should transform to ice XV above 100 K and back to ice VI above 129 K.[16] In that scenario a shift from 408 cm$^{-1}$ (vertical red line in Fig. 7b) to 338 cm$^{-1}$ (vertical green line) at 100–120 K and one from 338 cm$^{-1}$ to 402 cm$^{-1}$ at 130–140 K would be expected. Fig. 7b shows the heating development of that band up to 131 K. In that temperature range, the position slightly shifts from 408 cm$^{-1}$ to 403 cm$^{-1}$ without the occurrence of a band at 338 cm$^{-1}$ at any temperature. That indicates that the sample does not transform into ice XV upon heating. The small shift is consistent with the shift expected for thermal expansion of ice VI. That is, $D_2O$ ice VI remains both upon cooling at 1.8 GPa and heating at ambient pressure because the deuterons do not have enough time to order. That is, the $D_2O$ sample prepared by Rosu-Finsen and Salzmann was not given enough time for the deuterons to order and to reach the equilibrium structure that we regard to be ice β-XV. To actually make $D_2O$-ice β-XV will be the task for future work – and clearly

it will need a lot of patience to wait for the deuterons to order upon cooling at 1.8 GPa.

## Conclusion

We have investigated the question of how to clearly differentiate between a new H-ordered ice and deep glassy, H-disordered ice. Raman spectroscopy is a suitable choice to address this question since it probes for local H-order. In fact, we demonstrate that Raman spectroscopy is not only suitable to discriminate between H-order and H-disorder, as done in previous studies, but also to discriminate between distinct types of H-order. In the case of ice VI the question discussed diametrically in the literature is whether an order–order transition was experimentally realized by Gasser *et al.* as suggested by us[1] or whether instead a devitrification transition in H-disordered, glassy ice VI was realized as suggested by Rosu-Finsen and Salzmann.[16] In other words, the question is whether ice β-XV indeed represents a new H-ordered ice phase or needs to be reinterpreted as deep glassy, H-disordered ice VI. In the former scenario the phase diagram of $H_2O$ contains a stability area for this new phase below 103 K, whereas in the latter scenario the update reported in ref. 1 would be obsolete.

Raman experiments clearly speak in favour of the existence of H-ordered ice β-XV. Evidence for that conclusion is provided here based on four key experimental observations:

First, Raman spectra for ice β-XV, ice XV and ice VI prepared according to the literature protocol show that the spectrum of ice β-XV is neither equivalent to the Raman spectrum of ice VI nor ice XV. It can also not be constructed by a superposition of ice VI and ice XV spectra as would be expected in a scenario involving merely one H-ordered (ice XV) and one H-disordered phase (ice VI). Narrower bands and more substructures immediately suggest a higher degree of H-ordering in ice β-XV than in ice XV.

Second, we find that ice "XV" as known in the literature can in fact be regarded as a mixture of ice XV and ice β-XV domains. The Raman spectrum of ice "XV"$_{1.0GPa}$, prepared by slow cooling of ice VI at 1.0 GPa, can be considered as a superposition of ice β-XV and ice XV. While at low pressures ice XV is the favoured phase, it is ice β-XV at high pressures. At 0.0 GPa pure ice XV can be produced, whereas at 1.8 GPa ice β-XV forms rather than ice XV upon cooling. At intermediate pressures such as 1.0 GPa there is competition and domains of both H-ordered variants form. The ice β-XV fraction increases with pressure, which causes the continuous increase of the size of the first endotherm in DSC curves with increasing preparation pressure.[1] It also explains why recooling at $1.0 \times 10^{-6}$ GPa from 120 K improves the quality of ice XV: the ice β-XV domains formed next to the ice XV domains revert to ice XV/VI upon heating to 120 K at $1.0 \times 10^{-6}$ GPa, and then remain/transform to ice XV upon recooling.

Third, the spectra of ice β-XV reveal a loss of substructure upon heating, which implies a decrease of H-order. This is not consistent with the idea of glassy ice VI crystallizing above the glass transition temperature. In that scenario one would rather expect an increase of H-order. Analysis of the spectra based on the Whale-index, the OD-index and the librational index allows assessing the transition sequence incurred upon heating. This analysis demonstrates the transition sequence ice β-XV → ice XV → ice VI, with an order–order transition at $T_{o-o} \approx 103$ K and an order–disorder transition at $T_{o-d} \approx 129$ K.

Fourth, we reveal that the cooling rate has a decisive effect. While for slow cooling rates of 2 K min$^{-1}$ the H-ordering process takes place, only partial H-ordering takes place at rates of 20 K min$^{-1}$. Roughly 50% of the ice VI does not order at $1.0 \times 10^{-6}$ GPa upon cooling at 20 K min$^{-1}$ but persists even at the lowest temperatures. The time scale is also the crucial parameter for preparing $D_2O$-ice β-XV – and to have the opportunity to solve its crystal structure based on neutron diffraction experiments in the future. By decreasing the cooling rate at 1.8 GPa from $\approx 45$ K min$^{-1}$ to 1 K min$^{-1}$ the Raman spectrum changes considerably, where a librational band at 380 cm$^{-1}$ appears for the slowly cooled sample. This band is assigned to the librational band of $D_2O$-ice β-XV. However, the spectrum still contains additional bands that can be attributed to the presence of $D_2O$-ice VI and XV in this sample. We suggest that these domains will vanish at cooling rates much slower than 1 K min$^{-1}$ – with the possibility to form pure $D_2O$-ice β-XV in very slowly cooled samples.

Even though the Raman experiments massively speak in favour of the existence of ice β-XV and reveal it to be a highly ordered phase clearly distinct from ice XV, the idea of a "deep glassy state" can still be given some credit. Our work reveals that there is competition between two types of H-order upon cooling, where in some samples (especially the ones prepared near 1.0 GPa) domains of both types of H-order form. Two types of order parameters would then be required to describe the nature of the samples, where one order parameter has to describe the local order in the ice XV domains and the other has to describe the local order in the ice β-XV domains. While these samples are ordered locally, none of the two order parameters is able to describe the global order. It would then be possible to perceive the term "deep glassy state" as a mixture of locally ordered domains. However, for the slowly cooled 1.8 GPa $H_2O$ sample, we do not see evidence for the sample containing domains other than ice β-XV domains. Furthermore, an H-disordered state has also some relevance on the reaction coordinate converting ice β-XV to ice XV. The path from one ordered configuration to another ordered configuration necessarily has to pass through a disordered configuration. On this path the two H-ordered configurations represent energy minima, whereas the disordered configuration represents a saddle point. That is, the order–order transition at $\approx 103$ K has to pass through a transition state that is similar to ice VI. This transient ice VI could also be referred to as a deep glassy state. We therefore conclude that ice β-XV is a new phase, the crystal structure of which needs to be solved in the future. This, however, does not rule out the existence of deep glassy ice – under some experimental conditions such a state may indeed be encountered. The statement by Dennis D. Klug that

This journal is © the Owner Societies 2019

*Phys. Chem. Chem. Phys.*, 2019, **21**, 15452–15462 | 15461

"the search for new structures of ice will definitely continue"[26] cannot be more true!

## Conflicts of interest

There are no conflicts to declare.

## Acknowledgements

## Notes and references

1 T. M. Gasser, A. V. Thoeny, L. J. Plaga, K. W. Köster, M. Etter, R. Böhmer and T. Loerting, *Chem. Sci.*, 2018, **9**, 4224–4234.

2 E. Whalley, J. B. R. Heath and D. W. Davidson, *J. Chem. Phys.*, 1968, **48**, 2362–2370.

3 R. Howe and R. W. Whitworth, *J. Chem. Phys.*, 1989, **90**, 4450–4453.

4 C. G. Salzmann, P. G. Radaelli, J. L. Finney and E. Mayer, *Phys. Chem. Chem. Phys.*, 2008, **10**, 6313–6324.

5 J. J. Shephard and C. G. Salzmann, *Chem. Phys. Lett.*, 2015, **637**, 63–66.

6 E. Whalley, D. W. Davidson and J. B. R. Heath, *J. Chem. Phys.*, 1966, **45**, 3976–3982.

7 C. G. Salzmann, I. Kohl, T. Loerting, E. Mayer and A. Hallbrucker, *Phys. Chem. Chem. Phys.*, 2003, **5**, 3507–3517.

8 J. D. Bernal and R. H. Fowler, *J. Chem. Phys.*, 1933, **1**, 515–548.

9 P. W. Bridgman, *Proc. Am. Acad. Arts Sci.*, 1912, **47**, 441–558.

10 C. G. Salzmann, P. G. Radaelli, E. Mayer and J. L. Finney, *Phys. Rev. Lett.*, 2009, **103**, 105701.

11 G. P. Johari and E. Whalley, *J. Chem. Phys.*, 1979, **70**, 2094–2097.

12 K. W. Köster, A. Raidt, V. F. Landete, C. Gainaru, T. Loerting and R. Böhmer, *Phys. Rev. B*, 2016, **94**, 184306.

13 A. Rosu-Finsen and C. G. Salzmann, *J. Chem. Phys.*, 2018, **148**, 244507.

14 T. F. Whale, S. J. Clark, J. L. Finney and C. G. Salzmann, *J. Raman Spectrosc.*, 2013, **44**, 290–298.

15 C. G. Salzmann, B. Slater, P. G. Radaelli, J. L. Finney, J. J. Shephard, M. Rosillo-Lopez and J. Hindley, *J. Chem. Phys.*, 2016, **145**, 204501.

16 A. Rosu-Finsen and C. G. Salzmann, *Chem. Sci.*, 2019, **10**, 515–523.

17 B. Kamb, *Science*, 1965, **150**, 205–209.

18 W. F. Kuhs, J. L. Finney, C. Vettier and D. V. Bliss, *J. Chem. Phys.*, 1984, **81**, 3612–3623.

19 C. Knight and S. J. Singer, *J. Phys. Chem. B*, 2005, **109**, 21040–21046.

20 K. D. Nanda and G. J. O. Beran, *J. Phys. Chem. Lett.*, 2013, **4**, 3165–3169.

21 M. Del Ben, J. VandeVondele and B. Slater, *J. Phys. Chem. Lett.*, 2014, **5**, 4122–4128.

22 D. R. Moberg, P. J. Sharp and F. Paesani, *J. Phys. Chem. B*, 2018, **122**, 10572–10581.

23 J. L. Kuo and W. F. Kuhs, *J. Phys. Chem. B*, 2006, **110**, 3697–3703.

24 K. Komatsu, F. Noritake, S. Machida, A. Sano-Furukawa, T. Hattori, R. Yamane and H. Kagi, *Sci. Rep.*, 2016, **6**, 28920.

25 C. G. Salzmann, *J. Chem. Phys.*, 2019, **150**, 060901.

26 S. Sharp, Chem. World-UK, www.chemistryworld.com/news/study-challenges-hydrogen-ordered-ice-hypothesis/3010088.article, 2019.

27 K. Abe and T. Shigenari, *J. Chem. Phys.*, 2011, **134**, 104506.

28 T. Shigenari and K. Abe, *J. Chem. Phys.*, 2012, **136**, 174504.

29 C. G. Salzmann, A. Hallbrucker, J. L. Finney and E. Mayer, *Phys. Chem. Chem. Phys.*, 2006, **8**, 3088–3093.

30 C. G. Salzmann, A. Hallbrucker, J. L. Finney and E. Mayer, *Chem. Phys. Lett.*, 2006, **429**, 469–473.

31 We note a small difference in the librational range of ice $XV_{rec(120K)}$ shown here and ice $XV_{rec(130K)}$ presented in Fig. 8 from ref. 1: in addition to the band at 450 cm$^{-1}$ characteristic of ice XV also a weak band at 544 cm$^{-1}$ characteristic of ice VI appears for ice $XV_{rec(130K)}$.[1] This impurity of ice VI is not found in ice $XV_{rec(120K)}$ in Fig. 2. An explanation for the ice VI impurity in ice $XV_{rec(130K)}$ and its absence in ice $XV_{rec(120K)}$ will be given in Section 4.

32 V. Fuentes-Landete, K. W. Köster, R. Böhmer and T. Loerting, *Phys. Chem. Chem. Phys.*, 2018, **20**, 21607–21616.

15462 | *Phys. Chem. Chem. Phys.*, 2019, **21**, 15452–15462

This journal is © the Owner Societies 2019